Progress in Earth and Planetary Science

METHODOLOGY

Open Access

Single station bias calculation using data from calibrated GNSS station for various baseline distances

Muhammad Mubasshir Shaikh[1,2*]

Abstract

Precise ionospheric TEC can be derived from dual-frequency GNSS carrier phase leveled pseudorange measurements. However, differential code biases (DCB) of satellite and receiver are the main errors that cannot be ignored for precise TEC calculation. We have proposed a method of calculating station DCB using calibrated STEC data from a baseline GNSS station. The method is simply based on the understanding that the ionosphere observed by two baseline GNSS stations at the same universal time (UT) can be considered similar and would pose similar delay to the signals propagating to the two stations. The method is tested for different baseline distances of 250–1000 km and in different latitudinal regions. For 500 km baseline, the average DCB calculation error for one year data is less than 0.22 ns, 0.11 ns, and 0.25 ns for low, mid and high latitude regions, respectively. The most consistent results were obtained from high latitudes where the standard deviation remains less than 0.22 ns. The least accurate were the low latitude results where the spread of error were between 0.29 to 0.50 ns. Results showed that the accuracy and consistency of the DCB estimation reduced with the increasing baseline distance between the two participating GNSS stations. This was specifically true for low latitude regions.

Keywords Differential code bias, Single station bias, TEC calibration, GNSS

1 Introduction

The ionosphere is a dynamic region of the earth's atmosphere where conditions change diurnally and seasonally, particularly with reference to changes in space weather and geographical location. Total Electron Content (TEC) is an important parameter for understanding the spatial and temporal structures and variability of the ionosphere. TEC can be understood as the line integral of the electron density along the path of a radio signal. Since the launch of the Global Navigation Satellite System (GNSS), global coverage of the ionosphere has become a reality. Dual-frequency GNSS signals have been widely used to monitor and model the TEC across the globe (Jakowski et al. 2002). Precise ionospheric TEC can be derived from dual-frequency GNSS carrier phase and pseudorange measurements. However, inter-frequency satellite and receiver differential delay biases (IFBs) are the main errors that cannot be ignored for precise TEC calculation. These biases are also known as differential code biases (DCB). Previous studies show that DCBs are present due to the delays caused by the analog hardware of satellite and receiver and are instrumental (Lanyi and Roth 1988). Satellite and receiver DCBs combined could reach several tens of nanoseconds (ns) or approximately up to 100 TEC units (TECU); therefore, from GNSS measurements, DCBs must be removed for both satellite and receiver for precise positioning and accurate TEC calculation. Satellite and receiver DCBs are assumed to

*Correspondence:
Muhammad Mubasshir Shaikh
mshaikh@sharjah.ac.ae
[1] Sharjah Academy for Astronomy, Space Sciences & Technology, University of Sharjah, Sharjah, United Arab Emirates
[2] Department of Electrical Engineering, University of Sharjah, Sharjah, United Arab Emirates

be constant for a given time period, typically up to three days (Brunini et al. 2005).

Receiver DCB for a single station can typically be calculated by using polynomial of coordinates in solar-terrestrial reference system by the observations from a linear system of equations that is solved by least squares method for the polynomial coefficients and unknown biases (Lanyi and Roth 1988). Another widely used method to calculate a single station DCB is the method of minimization of the standard deviation of vertical TEC (VTEC) (Ma and Maruyama 2003). Apart from these commonly known methods, several other methods for GNSS DCB estimates using multi-frequency observations have been designed (Schaer 1999; Wang et al. 2016; Su et al. 2019). These methods successfully used various approaches to solve for the station DCB such as by setting the DCB as a constant during the TEC estimation or by decreasing the computation costs by using GIM (global ionospheric maps). Furthermore, several other techniques that help optimize the DCB estimation have been adopted such as optimization on DCB estimation based on regional or single station ionospheric modeling (Brunini and Azpilicueta 2010; Nie et al. 2018). However, all these methods come with some fundamental assumptions, for example, the single-layer TEC model, the assumption that the satellite and receiver DCBs remain constant for some days, and a Lagrange multiplier to separate the satellite and receiver DCBs generally called 'zero-mean constraint' etc. Using various methods mentioned above, several research institutes provide satellite and receiver DCB estimates in the form of IONEX (Ionosphere Map Exchange Format) file format. However, different DCB calculations provided from various institutes are not always in agreement with each other (Brunini et al. 2005). It is therefore understood that DCB estimation suffers similar shortcomings to TEC assumptions which are generally present in most of the sources through which we get the satellite and receiver biases.

We have proposed a simple technique for the computation of single station receiver DCB. The technique uses the model of STEC computed from the difference in GPS observables and does not depend on any of the assumptions made in previous works such as the use of TEC thin shell model, zero-mean constraint or requiring any external data such as GIM maps to help aid the DCB estimation process. The accuracy of DCB estimates is evaluated by the Chinese Academy of Sciences IONEX data files. In the next sections, a brief about the GNSS TEC calculation model is presented. 'Data' section presents the data sources used for the application and analysis of the proposed technique followed by the description of the proposed technique in the section 'DCB Calculation'. Performance of the technique is analyzed under 'Results and Analysis' section before concluding the paper with a brief summary and future work in 'Summary and Conclusion' section.

1.1 GNSS TEC model

Pseudorange measurements from dual-frequency GNSS receivers can be performed using time delay of GNSS signals at two different frequencies (Leick 2004). For dual-frequency GPS receivers, pseudorange measurements, P1 and P2, and carrier phase measurements, L1 and L2, are calculated at frequencies f1 (1.575 GHz) and f2 (1.227 GHz), respectively. The standard model for pseudorange and carrier phase measurements at f1 and f2 is:

$$P^{s}_{i,r} = R^{s}_{r} + c(\delta t_r - \delta t_s) + d^{s}_{trop,r} + d^{s}_{ion,i,r} + c\left(\mathrm{DCB_r} + \mathrm{DCB^s}\right) \quad (1)$$

$$L^{s}_{i,r} = \lambda_i \phi^{s}_{i,r} = R^{s}_{r} + c\left(\delta t_r - \delta t^{s}\right) + \lambda_i \phi^{s}_{ion,i,\,r} + \lambda_i \phi^{s}_{trop,r} - c\left(\mathrm{DCB_r} + \mathrm{DCB^s}\right) + \lambda_i N^{s}_{i} \quad (2)$$

where 'i' denotes the index for frequency, 'r' is receiver index, 's' is satellite index, 'R' is the actual range between satellite and receiver, 'λ' and 'ϕ' are wavelength and phase delay, respectively, '$\delta t'_r$' and 'δt_s' are the clock errors for the receiver and satellite, respectively, '$d^{s}_{trop,r}$' and '$d^{s}_{ion,i,r}$' are the troposphere and ionosphere group delays, respectively, '$\mathrm{DCB_r}$' and '$\mathrm{DCB^s}$' are the frequency-dependent receiver and satellite differential code biases, respectively, and 'N' is the initial phase ambiguity. The STEC using code and phase delay observations can be obtained by using the geometry-free linear combination by ignoring the higher order effects of the ionosphere as follows:

$$P_I = 40.3\left(\frac{f_1^2 - f_2^2}{f_1^2 * f_2^2}\right)\mathrm{STEC}^{s}_{r} - c\left(\mathrm{DCB_r} + \mathrm{DCB^s}\right) \quad (3)$$

$$L_I = 40.3\left(\frac{f_1^2 - f_2^2}{f_1^2 * f_2^2}\right)\mathrm{STEC}^{s}_{r} - c\left(\mathrm{DCB_r} + \mathrm{DCB^s}\right) + \Delta N^{s} \quad (4)$$

where 'P_I' and 'L_I' are the ionospheric geometry free linear combinations for code and phase observations, respectively, 'STEC' is slant total electron content between each satellite-to-receiver link. Although unlike code delay measurements, carrier phase measurements are less prone to measurement noise and multipath, they are biased by phase ambiguity (Mannucci et al. 1998). Carrier-to-code leveling algorithm (Ciraolo et al. 2007) is widely used to reduce the ambiguities from the carrier phase ionospheric observables. After obtaining ionospheric observables, as

mentioned in (3) and (4), the average of the differences between them is computed for every continuous arc as:

$$\langle L_I - P_I \rangle_{\text{arc}} = \frac{1}{N} \sum_{1}^{N} (L_I - P_I) \tag{5}$$

where '*N*' is the number of continuous measurements contained in a single satellite-to-receiver arc. The subscript 'arc' refers to every continuous set of carrier phase observations between the receiver and a particular satellite (i.e., a group of consecutive observations along which the ambiguities on L1 and L2 do not change). Finally, to obtain the leveled STEC phase observations:

$$\tilde{L}_{I,\text{arc}} = L_{I,\text{arc}} - \langle L_{I,\text{arc}} - P_I \rangle_{\text{arc}} \tag{6}$$

where '$\tilde{L}_{I,\text{arc}}$' is the carrier phase ionospheric observable leveled to the code-delay ionospheric observable. This procedure is known as carrier-to-code levelling process. Using the above-mentioned carrier-to-code levelling processes, in this work, a simple technique is introduced which could help calculate the receiver DCB provided that the leveled STEC data from a baseline station is available. A detailed description of the proposed technique is given in the section DCB Calculation.

1.2 Data

All the GNSS data including RINEX (Receiver Independent Exchange Format) and IONEX data used in this study has been acquired from NASA's Crustal Dynamics Data Information System (CDDIS: https://cddis.nasa.gov/archive/gnss/) database. The data period used in this study is of the year 2019 since it is the low solar activity year. Only data from GPS constellation has been used in this work. Initially, we considered using data from 64 IGS stations from different latitudinal regions. However, since, we have only considered GPS P-code data in this work, the number of GNSS stations we ended up using in this work are 19. This gives us 11 different combinations with different baseline distances in pairs of GNSS stations with which we have tested our technique. Data observed on days with active geomagnetic conditions, that is, Dst < -50 nT and Kp > 3 have not been considered for analysis. The Dst index has been obtained from World Data Center (Kyoto et al. 2015) and Kp from GFZ Data Services (Matzka et al. 2021). The minimum elevation mask for GPS observations used in this work is 30°.

2 Method

The proposed method to estimate the station DCB is simply based on the understanding that the ionosphere observed by two baseline GNSS stations at the same universal time (UT) can be considered similar and would pose similar delay to the signals propagating to the two stations. That is, if a particular GNSS satellite is visible to two different GNSS stations present at a certain baseline at the same UT, their average STEC, calculated using overlapping STEC arcs, considered as same. In this way, uncalibrated STEC data for which the receiver DCB is unknown can be calibrated using the calibrated STEC data from the other baseline GNSS station and the difference of their STEC can be used to calculate DCB for uncalibrated station. STEC arc here is referred to the STEC data calculated using continuous observation between a GNSS station and a GNSS satellite. The term baseline is understood here as the straight-line distance between the two participating stations, that is, the uncalibrated GNSS station for which DCB is being calculated and the calibrated GNSS station from which the data is taken for the DCB calculation process. For the calibrated GNSS station, the STEC data is code-to-phase leveled as indicated in (6). The station from which the calibrated STEC is obtained will be referred to as 'Ref'.

Figure 1 (top panel) shows two arcs overlapping in time observed by two different GNSS stations MAL2 and MBAR. Station MAL2, used here as Ref, is calibrated for satellite and receiver biases available from IONEX files and leveled through carrier-to-code leveling process using (3), (4) and (6). Station MBAR is only corrected for the satellite biases available from the same source of IONEX data. Since the arc observed by station MAL2 is longer in time than the arc observed by station MBAR, we have only considered the length of the arcs from the two stations which are overlapping in time as shown in Fig. 1 (middle panel). These two arcs overlapping in time will be referred to as 'overlapping arcs'. The bias between the two overlapping arcs is then calculated by taking the mean of the difference of the two overlapping arcs. This will be referred to as 'arc bias' and calculated as shown below:

$$\text{arc bias} = L_{I,\text{arc,uncalib}} - \left\langle L_{I,\text{arc,uncalib}} - \tilde{L}_{I,\text{arc}} \right\rangle_{\text{arc}} \tag{7}$$

where '$L_{I,\text{arc,uncalib}}$' is the uncalibrated phase arc for which the DCB calculation is being performed, '$\tilde{L}_{I,\text{arc}}$' is the calibrated phase arc of Ref calculated using (6).

Figure 1 (bottom panel) shows how the two overlapping arcs look like after the arc bias is removed from the uncalibrated arc. The process is then repeated for the calculation of all arc biases using all the overlapping arcs of STEC for all available GNSS satellites observed by the two participating stations in a 24-h period. Finally, the station bias is calculated by taking an average of all the arc biases. This daily station bias calculation in TEC unit (TECU) is then divided by 2.86 to convert it to

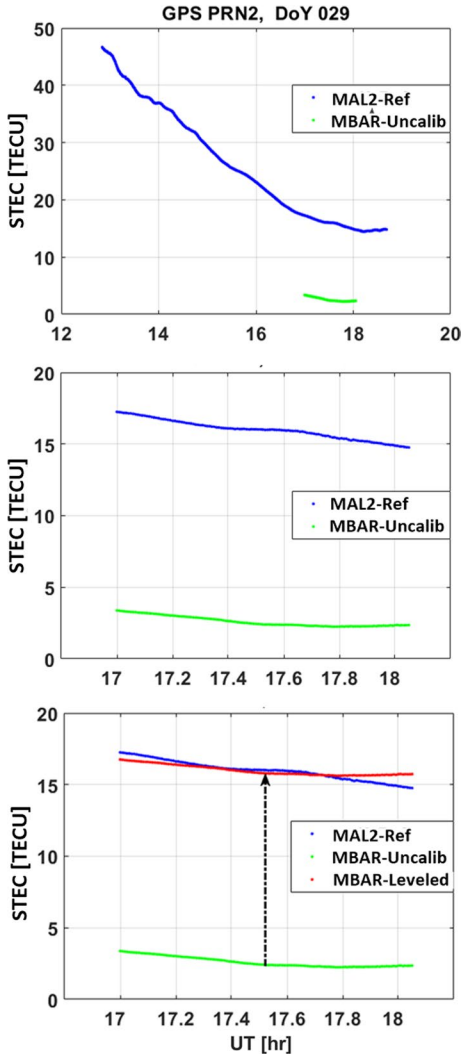

Fig. 1 Calibration of overlapping STEC arcs of the two participating stations used to calculate the station bias. The data shown is STEC arcs obtained from GPS PRN02 on day of year 029. Please note the changing *x*- and *y*-axis in separate panels. Please note that the scale of x- and y-axes are different in each panel

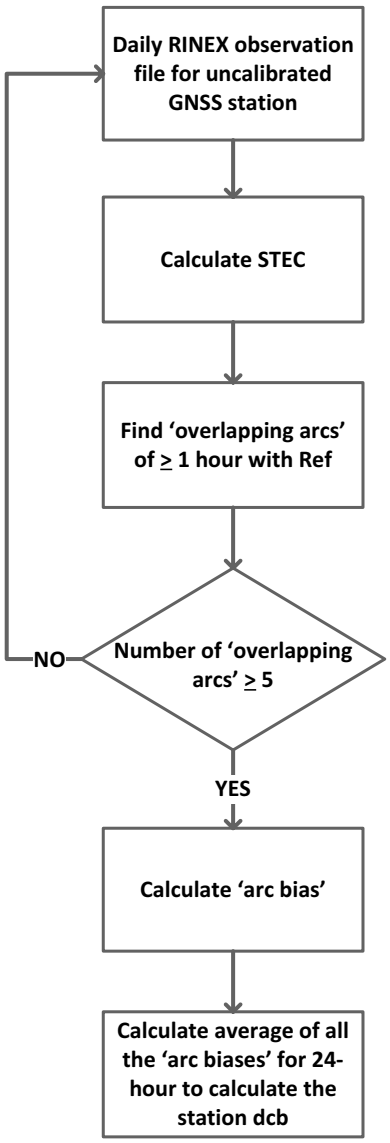

Fig. 2 Simplified block diagram for the proposed technique to calculate bias for the uncalibrated GNSS station

nanoseconds (ns). While applying this technique, we have used a minimum length of the overlapping STEC arcs greater than or equal to 1 h and minimum of 5 such overlapping arc must be available for the daily GNSS station bias calculation. These limits are set on the basis of trial and error. In case of more than one overlapping arcs present from a particular satellite, referred here as 'sub-arcs', an average of all the individual overlapping sub-arcs' biases are used to calculate the arc bias. Figure 2 shows a simplified block diagram of the proposed technique. In this work, we have considered several different baseline distances between the uncalibrated station and the Ref. These baseline distances are varying around 250 km to 1000 km and their results are presented in the next section.

3 Results

We have selected several pairs of GNSS stations from different latitudinal regions to test this method. This was done to check the validity and robustness of the method in different latitudinal regions and for different baseline distances. It was desired that the technique should be simple enough to be implemented quickly and effectively without the need of a complicated algorithm or assumptions. While selecting the GNSS stations, it was preferred that different baseline distances of greater than 500 km

are selected for the test and analysis. This is important since there is a limitation of minimum of 5 overlapping arc be present between both stations on the day on which the DCB calculation is desirable.

Figure 3 shows the DCB estimation error (Δ DCB) calculated between daily bias estimation using the proposed method and the bias available from the IONEX files provided by the Chinese Academy of Sciences (file code casg in CDDIS). Here, only results concerning stations with baseline distances of approximately 500 km are shown. It can be seen that the proposed technique estimated the DCB accurately at different latitudinal sectors. Particularly, in mid-latitudes, the average error is only limited to 0.04–0.11 ns compared to what was estimated in the IONEX files. The results from the higher latitudes are very consistent for the whole 1-year period, which can be seen by the small spread of error as shown in the bottom panel of Fig. 3.

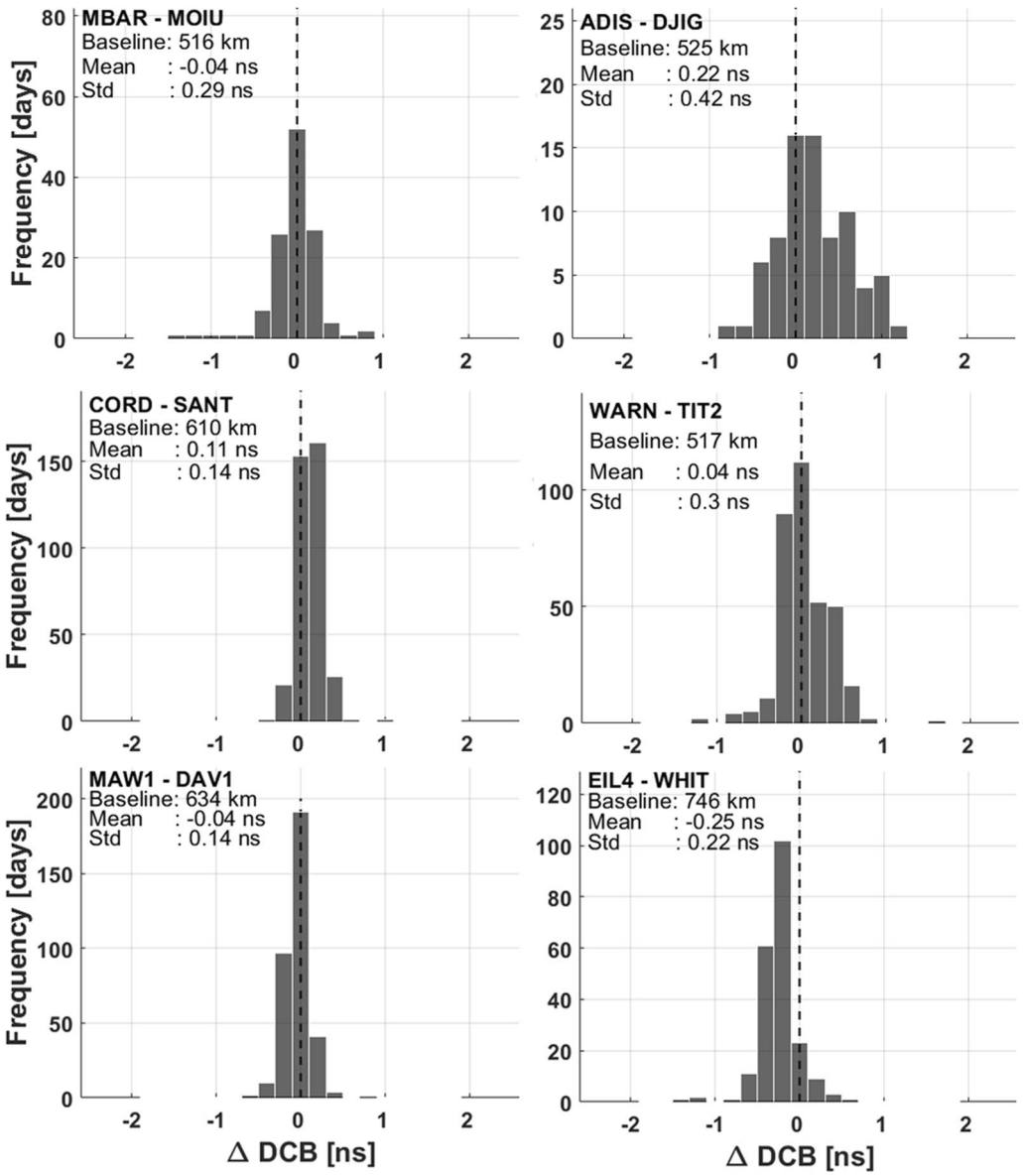

Fig. 3 For low-, mid-, and high-latitude station bias calculation. Top row shows results for low-latitude, middle one for mid-latitude and bottom one for high latitude stations, respectively. Participating station pair's codes are shown in the top left corner of each panel. Baseline distance between the two participating stations, mean and standard deviation of calculation errors are also shown at the top left corner. The frequency axis on each plot is different and set according to the number of days' data available. The black dotted line in the middle of each plot shows the zero difference line between calculated and available station bias

Even though the baseline distances are larger in higher latitude stations, the results are still consistent as compared to low- and mid-latitude stations. It is also noted that bias calculation for southern hemispheric stations seems to be more consistent as compared to the northern hemispheric stations, as shown in the left column of Fig. 3.

Apart from testing the algorithm for a minimum baseline distance of 500 km, we have also checked whether the technique also works with other baseline distances. As one of our two special cases, we also checked if the technique generally performs better or at least equally good if the baseline distance is smaller. Figure 4 is an example of two pairs of stations where baseline distances are approximately half of what was used in Fig. 3. Figure 4 clearly shows that the technique performs better when the baseline distances are smaller. This may be due to the fact that with more overlapping arcs and closer ionospheric conditions due to shorter geographical distances, the overall average of the day for the station DCB calculation improves significantly. Specifically, the spread of the error is limited to only 0.17–0.18 ns in both mid- and high-latitudes as compared to 0.14–0.30 ns in case of 500 m baseline for mid- and high-latitude stations' pairs as shown in Fig. 3. It was desired that at least on low-latitude pair is tested for this shorter baseline case, but unfortunately, the data is not available.

A second special case for longer baseline distances has also been tested. Figure 5 is the DCB calculation for a baseline distance at least twice the baseline previously used in Fig. 3. The bias calculation error has certainly deteriorated in low- and high-latitude in terms of average and spread of error calculation, respectively. However, the calculation of average bias for low latitude stations' pair has shown remarkable results with an error less than 0.1 ns. The best bias calculation results are again obtained in the mid-latitudes, where the technique produces a similar error as it was in the case of

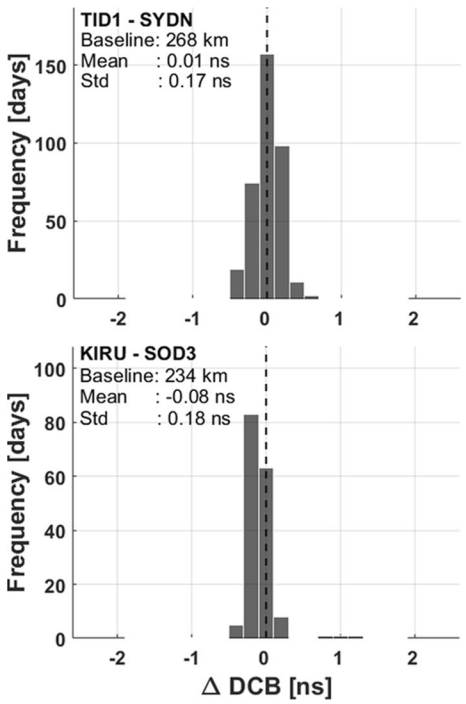

Fig. 4 Bias calculation error for shorter baseline case. The top panel is for mid-latitude and the bottom panel is for the high-latitude stations' pair. The black dotted line in the middle of each plot shows the zero DCB error line

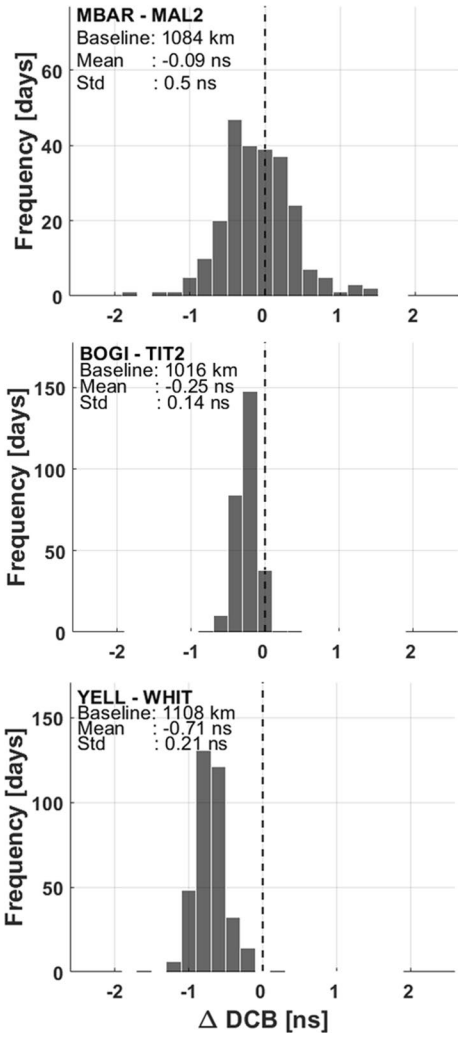

Fig. 5 Bias calculation error for longer baseline case. Top row shows results for low-latitude, middle one for mid-latitude and bottom one for high latitude stations' pair. The black dotted line in the middle of each plot shows the zero DCB error line

the 500 km baseline. The spread of error over a one-year period is also less than 0.15 ns.

4 Discussion

Considering all the results, it has been concluded that the proposed technique based on overlapping arcs of two baseline stations can be effectively used to calculate the station bias for the uncalibrated station. The maximum errors in DCB calculation for the 500 km baseline is found to be 0.25 ns at high latitude. The standard deviation shows that the maximum spread ΔDCB calculation is also limited to an average value of 0.35 ns which is found in low latitude. Two other baseline distances were evaluated to check the robustness of the technique. For half baseline case for which baseline distance between the two stations was limited to approximately 250 km, the results seemed to improve. The average ΔDCB is found to be 0.01 and 0.08 in mid- and high-latitude stations, respectively. The spread of the error is also limited to 0.17–0.18 ns for mid- and high-latitude stations' pair, respectively. The second special case considered where the baseline distance is increased to at least double the 500 km baseline, that is, approximately 1000 km. Mid-latitude stations' pairs were most consistent with 0.25 ns average error and spread of only 0.14 ns. Although, ΔDCB calculation was found to be least in low-latitude as 0.09 ns, the consistency is much worse than mid-latitude, that is, 0.50 ns. The high-latitude DCB calculation was the least accurate among the three with 0.71 ns average. However, the calculations were consistent with only 0.21 ns spread.

Table 1 shows an overall summary of different GNSS station pairs used in this work with their geographical regions and approximate baseline distances mentioned. The data shown in the table has been taken from different panels of Figs. 3, 4, 5. The results obtained from several pairs of GNSS stations separated by different baseline distances showed that the method works accurately. Specifically, for mid-latitudes stations, the error in calculating station DCB remains less than or equal to 0.11 ns, on average, for less than 500 km baseline distance, when compared to the available IONEX data taken from the same source with which the STEC is calibrated for the Ref. It increased to 0.25 when the baseline increased to more than 1000 km. For low-latitude GNSS stations, the maximum error remains less than 0.22 ns at all baseline distances. For high-latitude stations, the mean error systematically increased with the baseline distance from 0.08 to 0.71, respectively. The most consistent results were obtained from high latitudes where the standard deviation ranges between 0.14 to 0.22 ns. The least accurate were the low latitudes results where the spread of error were between 0.29 to 0.50 ns. It has been inferred from the results that, in general, the accuracy and consistency of the DCB calculation reduce with the increasing baseline. This is specifically true for low-latitude GNSS stations.

The results obtained after applying a very simple technique of utilizing overlapping STEC arcs using calibrated data from a baseline station seems to be producing the desired results consistently in all latitudinal regions. It is also understood that the technique can be effectively applied to calculate reliable results with baseline distances of less than 1000 km in all latitudinal regions without any complex mathematical algorithms for averaging or extrapolating the results. It should not be wrong to conclude that the method works accurately if the baseline distance between the two participating stations remains less than or close to 500 km.

Table 1 Pair of GNSS stations used to evaluate the technique. In the stations' pair, in the first column, the first station code is the code of the uncalibrated station, and the second code is for the Ref

SN	GNSS station pair	Baseline distance (km)	DCB error mean (ns)	DCB error standard deviation (ns)	Region
1	MABR-MOIU	516	− 0.04	0.29	Low-Lat
2	ADIS-DJIG	525	0.22	0.42	Low-Lat
3	MBAR-MAL2	1084	− 0.09	0.50	Low-Lat
4	TID1—SYDN	268	0.01	0.17	Mid-Lat
5	CORD-SANT	610	0.11	0.14	Mid-Lat
6	WARN-TIT2	518	0.04	0.30	Mid-Lat
7	BOGI-TIT2	1016	− 0.25	0.14	Mid-Lat
8	KIRU-SOD3	234	− 0.08	0.18	High-Lat
9	MAW1-DAV1	635	− 0.04	0.14	High-Lat
10	EIL4-WHIT	745	− 0.25	0.22	High-Lat
11	YELL-WHIT	1108	− 0.71	0.21	High-Lat

5 Conclusions

We have proposed a technique to calculate GNSS station DCB for TEC calibration. Among all the other techniques currently in use, this technique is very simple to apply and does not depend on any of the assumptions such as the use of the ionospheric thin shell model, zero-mean constraint or requiring any external data such as GIM maps to help aid the DCB estimation process. The purpose of the technique is to provide a quick way to calculate the station DCB for any GNSS station which is within baseline distance of 250–1000 km from a calibrated GNSS station. The proposed method is simply dependent on the availability of calibrated STEC data from a baseline GNSS station. The technique works by finding 'overlapping arcs' of STEC between the baseline uncalibrated and Ref stations and then calculating the 'arc bias' for each overlapping arc of at least 1 h duration. It is required that, for the calculation of daily station DCB, at least 5 of such overlapping arcs must be present between the two baseline stations in a 24-h period. To have better accuracy, it is strongly recommended that the calibrated STEC data is also code-to-phase leveled. Although we have only used GPS data in this work, it is believed that the proposed technique could be effectively used to calculate station DCB using data from other GNSS constellations.

The proposed technique provides an alternate method of calculating single station DCB without the complication of previously applied assumptions or using external data. A comprehensive analysis has been done by applying the technique with several pairs of GNSS stations at different latitudinal sectors to check the validity and consistency of the technique. The results show that the technique works accurately and consistently up to 1000 km baseline distance. The technique may also work for larger baseline distances but with lesser accuracy and consistency. This work will be continued in expanding the scope of the application of this technique with other GNSS constellation and to improve the precision and accuracy. Specifically, it would be interesting to see if the short-term receiver DCB variability as mentioned by Zhang et al. (2019) would impact the outcome of the results presented in this paper.

Abbreviations

CDDIS	Crustal dynamics data information system
DCB	Differential code bias
GIM	Global ionospheric map
GNSS	Global navigation satellite system
IFB	Inter-frequency bias
IONEX	Ionosphere map exchange format
STEC	Slant total electron content
PRN	Pseudorandom noise
RINEX	Receiver independent exchange format
TEC	Total electron content
TECU	Total electron content unit
UT	Universal time
VTEC	Vertical total electron content

Acknowledgements

Author would like to thank International GNSS Service (IGS) for providing a comprehensive information about the network of GNSS station which helped in the selection of GNSS stations used in this work. Author is grateful for the CDDIS (https://cddis.nasa.gov/archive/gnss/) database for providing global RINEX and IONEX data free of charge for scientific use.

Authors' Information

Dr Mubasshir is currently working as a research associate and principal investigator at the Space Weather and Ionosphere (SW&I) laboratory at Sharjah academy for Astronomy, Space Sciences and Technology (SAASST), Sharjah, UAE. Before joining SAASST, he completed his doctorate from Politecnico di Torino, Italy, in the research area of ionospheric physics. He then worked as a postdoctoral visiting research scientist at the Abdus Salam International Center for Theoretical Physics (ICTP), Trieste, Italy. His research interests include ionospheric modeling and data assimilation techniques for ionospheric empirical modeling.

Author contributions

MMS initiated the idea, designed the methodology, analyzed the data and wrote the complete manuscript. The author read and approved the final manuscript.

Funding

No external has been received to conduct the research presented in this paper.

Availability of data and materials

The RINEX and IONEX data used to perform this research work has been obtained from CDDIS database at: https://cddis.nasa.gov/archive/gnss/.

Declarations

Competing interests

The authors declare that they have no competing interest.

Received: 1 September 2022 Accepted: 29 December 2022
Published online: 09 January 2023

References

Brunini C, Azpilicueta FJ (2010) GPS slant total electron content accuracy using the single layer model under different geomagnetic regions and ionospheric conditions. J Geod 84:293–304. https://doi.org/10.1007/s00190-010-0367-5

Brunini C, Meza A, Bosch W (2005) Temporal and spatial variability of the bias between TOPEX- and GPS derived total electron content. J Geod 79:175–188. https://doi.org/10.1007/s00190-005-0448-z

Ciraolo L, Azpilicueta FJ, Brunini C, Meza A, Radicella SM (2007) Calibration errors on experimental slant total electron content (TEC) determined with GPS. J Geod 81:111–120. https://doi.org/10.1007/s00190-006-0093-1

Jakowski N, Heise S, Wehrenpfennig A, Schlüter S, Reimer R (2002) GPS/GLONASS-based TEC measurements as a contributor for space weather forecast. J Atmos Solar Terr Phys 64(5):729–735. https://doi.org/10.1016/S1364-6826(02)00034-2

Lanyi GE, Roth T (1988) A comparison of mapped and measured total ionospheric electron content using Global Positioning System and beacon satellite observations. Radio Sci 23(4):483–492. https://doi.org/10.1029/RS023i004p00483

Leick A (2004) GPS satellite surveying, 3rd edn. Wiley, Hoboken, N. J.

Ma G, Maruyama T (2003) Derivation of TEC and estimation of instrumental biases from GEONET in Japan. Ann Geophys 21:2083–2093. https://doi.org/10.5194/angeo-21-2083-2003

Mannucci AJ, Wilson BD, Yuan DN, Ho CH, Lindqwister UJ, Runge TF (1998) A global mapping technique for GPS derived ionospheric total electron content measurements. Radio Sci 33(3):565–582. https://doi.org/10.1029/97RS02707

Nie W, Xu T, Rovira-Garcia A, Juan JM, Subirana JS, González-Casado G, Chen W, Xu G (2018) Revisit the calibration errors on experimental slant total electron content (TEC) determined with GPS. GPS Solut 22:85. https://doi.org/10.1007/s10291-018-0753-7

Schaer S (1999) Mapping and predicting the earth's ionosphere using the global positioning system. Geod. Geophys. Arb. Schweiz 59.

Su K, Jin S, Hoque MM (2019) Evaluation of ionospheric delay effects on multi-GNSS positioning performance. Remote Sens 11(2):171. https://doi.org/10.3390/rs11020171

Wang N, Yuan Y, Li Z, Montenbruck O, Tan B (2016) Determination of differential code biases with multi-GNSS observations. J Geod 90:209–228. https://doi.org/10.1007/s00190-015-0867-4

Zhang B, Teunissen PJG, Yuan Y, Zhang X, Li M (2019) A modified carrier-to-code leveling method for retrieving ionospheric observables and detecting short-term temporal variability of receiver differential code biases. J Geod 93:19–28. https://doi.org/10.1007/s00190-018-1135-1

Publisher's Note